MNF Education

Keywords:
Bioreactor / 4-Decanolide / Downstreaming / Lactoferrin / Mass balances / Membrane adsorber / Scale-up calculations / Similarity theory

Received: December 17, 2004; revised: March 1, 2005; accepted: March 4, 2005

Scale-up of natural product formation and isolation

Ralf G. Berger, Thomas Scheper and Karl Schügerl

Zentrum Angewandte Chemie, Universität Hannover, Hannover, Germany

Introduction

All investigations on microbial product formation start on small scales, *i. e.*, on Petri dish or Erlenmeyer flask dimensions. Arrays of small bioreactors operated in parallel mode may be used to improve the composition of the cultivation medium, to establish optimal conditions of temperature and pH-value of the medium, and to assess critical concentrations of key components of the medium, such as precursor substrate. Dissolved oxygen is commonly evaluated in small (stirred tank) reactors. The constant aim of a scale-up from laboratory to a large industrial-scale reactors is to attain maximum biological performance using a minimum of time and resources. A number of different bioprocesses run on very large scales, for example, to produce small (ethanol), medium-sized (penicillin), or large molecules (single cell protein), or to treat high-volume industrial streams of substrate (sewage, bioleaching). The importance of further developing traditional bioprocesses in the field of food biotechnology was emphasized recently [1].

Volatile flavors, such as vanillin, menthol, benzaldehyde, fruit esters, and 'green note' compounds, belong to the most valuable compounds in food formulations. Their biotechnological production was studied in various types of bioreactors [2, 3]. One of the problems of this recent branch of novel bioprocesses is that the requirement of the usually used microorganisms for oxygen and the volatility of the target compound present a conflict of interest (sufficient aeration *vs.* loss of product) typical of many scale-up steps. Like ethanol, many volatile compounds are highly toxic to their producer cells. This calls for efficient downstream options for treating large volumes of highly dilute and heterogeneous solutions.

The intelligent downstreaming of agricultural raw materials offers the possibility to gain valuable products from these easily available and well-accepted resources. In Germany over ten million tons of whey are produced every year. Major whey proteins are α-lactalbumin, β-lactglobulin, BSA, and bovine immunoglobulin G (IgG). Up to now the major products from whey are whey powder, lactose, and whey protein concentrates. Minor high value proteins are lactoperoxidase and lacto(trans)ferrin, beside other minor compounds. The concentration of these valuable compounds is in the range of 20–100 mg/L. The following sections present the theoretical basis for scale-up, the development of a bioprocess for the generation of a volatile flavor, the development of an efficient downstreaming process for transferrin from a biomedium, and rules and strategies to accelerate the experimental steps of scaling-up and downstreaming.

Fundamentals for scale-up

Chemical elementary balances

Chemical elemental balances are used to relate the (specific) consumption and formation rates of various components during the cultivation and production stages. The carbon balance is the most important of them. In an initial stage it can be used to find out relations between the various rates. If the individual components in the medium which contain C-atoms are labeled S_i^K(substrate component), P_j^K (product component), and X^K (cell mass component), and the C-content (g/g) in these components is referred to as a_{Si}, a_{Pj}, and a_X, respectively, then the C-balance can be written as

$$\sum a_{Si}R_{Si} = a_X R_X + \sum a_{Pj}R_{Pj} \qquad (1)$$

The C-balance becomes with

Correspondence: Dr. Ralf G. Berger, Institut für Lebensmittelchemie im Zentrum Angewandte Chemie der Universität Hannover, Wunstorfer Straße 14, D-30453 Hannover, Germany
E-mail: rg.berger@lci.uni-hannover.de
Fax: +49-511-7624547

R_{Si} = consumption rate of substrate
R_X = growth rate
R_{Pj} = product formation rate

$\sigma_i = \frac{R_{Si}}{X}$ specific consumption rate of the substrate (1/h)

$\mu = \frac{R_X}{X}$ specific growth rate (1/h)

$\pi_J = \frac{R_{Pj}}{X}$ specific formation rate of product *j* (1/h)

specific consumption rate of the substrate (1/h)

$$\sum_{i=1}^{n} a_{Si}\sigma_i = a_X\mu + \sum_{j=1}^{m} a_{Pj}\pi_j \qquad (2)$$

The calculation can be simplified by assessing the main substrate (*e.g.*, glucose) and the minor substrates (yeast extract, corn steep liquor, pharma media) separately.

$$\sum_{i=1}^{n} a_{Si}R_{Si} = a_S R_S + a_S^* R_S^*$$
$$\sum_{i=1}^{n} a_{Si}\sigma_i = a_S\sigma + a_S^*\sigma^* \qquad (3)$$

in which a_S is the C-content of the main substrate (g/g), a_S^* is the main C-content of the secondary substrates (g/g), $-\sigma$ is the specific rate of the main substrate consumption (g/L), and $-\sigma^*$ is the mean specific rate of the secondary substrate consumption (g/h).

A further assumption is that only two products are formed, product *P* with a rate of formation R_P or π_P and a C-content a_B and CO_2, represented by R_{CO_2} or π_{CO_2} and a_{CO_2}. The C-content of cell mass a_X is determined by experiment. Similar balances can be set up for other elements, such as hydrogen, oxygen, sulfur, nitrogen, or phosphorus.

The yield coefficients are defined as the relationships between the (specific) consumption and production rates, if the maintenance (m_S) of the cells is neglected:

$$-Y_{S/X} = \frac{R_X}{-R_S} = \frac{\mu}{-\sigma}$$

substrate yield coefficient for the growth (g/g)

$$-Y_{S/X}^* = \frac{\mu}{-\sigma^*}$$

secondary substrate yield coefficient for the growth (g/g)

From the oxygen balance we obtain:

$$-Y_{O/X} = \frac{R_X}{-R_O} = \frac{\mu}{-\theta}$$

oxygen yield coefficient of the growth (g/g)

in which $-R_O$ is the oxygen consumption rate (g/h) at a specific growth rate (1/h) and $-\theta = \frac{R_O}{X}$ is the specific oxygen consumption rate (1/h).

The yield coefficients of the main product are

$$-Y_{P/S} = \frac{-R_S}{R_P} = \frac{-\sigma}{\pi}$$

yield coefficient of substrate for the product

$$-Y_{P/S}^* = \frac{-R_S^*}{R_P} = \frac{-\sigma^*}{\pi}$$

yield coefficient of secondary substrate for the product

$$-Y_{P/O} = \frac{-R_O}{R_P} = \frac{-\theta}{\pi}$$

yield coefficient of oxygen for the product.

The second product is CO_2. R_{CO_2} is the CO_2 production rate (g/h). $\pi_{CO_2} = \frac{R_{CO_2}}{X}$ is the specific CO_2 production rate (1/h).

Continuous and accurate measurements of both oxygen and carbon dioxide in the waste gas stream is provided by modern gas analyzers based on paramagnetism or infrared absorption, and back-transmission of the actual data to a control system may be used to run the bioprocess under equilibrium conditions [4].

If the atomic compositions of the cell mass, substrates, and products are known, cell growth and product formation can be balanced by means of the composition of the chemical components. This yields a 6×10-matrix consisting of six atomic elements (C, H, O, N, S, P) with ten different medium components (cell mass, substrate, product, carbon, nitrogen, oxygen, sulfur, phosphorus source, water, and CO_2). In addition the molar enthalpies and molar conversion rates of the medium components allow to calculate heat balances for growth and product formation by means of the difference of the molar mass and enthalpy flows entering into and leaving the system. The theoretical limits of yield coefficients $Y_{X/S}$ and $Y_{X/O}$ can be evaluated from these balances [5].

Formal kinetics and reactor balances

Several relationships describe cell growth. Monod's specific growth rate is

$$\mu = \mu_{max}\frac{S}{S + K_S} \qquad (4)$$

in which μ_{max} is the maximum specific growth rate (no limitation by substrates, oxygen) (1/h), *S* is the substrate concentration (g/L), and K_S is a model parameter or saturation constant of substrate (g/L).

For high substrate concentration in comparison with K_S, $\mu \approx \mu_{max}$ holds true.

For very low substrate concentration in comparison with K_S a linear relationship prevails between μ and S:

$$\mu = \mu_{max} \frac{S}{K_S} \tag{4a}$$

The relationship between the product formation rate (R_P) and the growth rate (R_X) is

$$\begin{aligned} R_P &= \alpha R_X + \beta \\ X\pi &= \alpha\mu + \beta \end{aligned} \tag{5}$$

in which α and β are constants. The product formation rate is given by

$$R_P = \frac{\mu_{max} X}{Y_{P/X}} \text{ where } Y_{P/X} = \frac{R_X}{R_P} \tag{6}$$

2.2.1 Growth in an idealized reactor

A) For nonlimited growth in an ideally mixed stirred tank reactor

$$R_X = \mu_{max} X \tag{7a}$$

holds true. With the initial condition $X = X^o$ for $t = 0$ this relationship yields

$$X = X^O \exp\ (\mu_{max} t) \tag{8a}$$

The rate of substrate and oxygen consumption can be calculated from the growth rate and corresponding yield coefficients (Table 1):

$$-R_S = -\frac{\mu X}{-Y_{S/X}} \text{ and } q_S = \frac{-R_S}{X} \tag{7b}$$

$$-R_O = \frac{\mu X}{-Y_{O/X}} \text{ and } q_O = \frac{-R_O}{X} \tag{7c}$$

B) The mass balance for nonlimited growth in an ideally mixed continuously operated reactor is under steady-state condition

$$\frac{dX_1}{dt} = \mu_{max} X_1 - D(X_1 - X_0) = 0 \tag{9a}$$

$X_0 = 0$ applies if the medium feed is cell-free.

$$D = \frac{V}{V_R} = \frac{1}{\tau}$$

is the dilution rate of the medium, V is the volumetric flow rate (m^3/h), and V_R is the reactor volume (m^3), τ (h) is the mean residence time of the medium in the reactor.

$\mu_{max} = D$ for $X_o = 0$

Table 1. Typical parameters of some microorganisms with glucose as substrate

	μ_{max} (h^{-1})	$Y_{S/X}$ ($g \cdot g^{-1}$)	$q^*_{S\,max}$ ($mmol \cdot g^{-1}h^{-1}$)	q^*_O ($mmol \cdot g^{-1}h^{-1}$)
Escherichia coli (B/r)	1.36		3.8	25
Escherichia coli (K)i	0.55		0.95	12.5
Bacillus subtilis	0.95		1.1	
Saccharomyces cerevisiae (monoauxic, anaerobic)	0.30	0.1		
Saccharomyces cerevisiae (diauxic, aerobic)	0.47	0.5	3.5	8
Trichosporon cutaneum	0.40	0.5	0.9	9
Candida tropicalis	0.67	<0.5	8	12–14

C) For batch cultivation of substrate and/or oxygen-limited growth in an ideally mixed stirred tank reactor.

$$R_X = \mu X \text{ with } \mu = \mu_{max} \frac{S}{S + K_S} \tag{4}$$

for substrate-limited growth

$$\mu = \mu_{max} \frac{O}{O + K_O} \text{ for oxygen-limited growth} \tag{10}$$

$$X = X^O \exp\ (\mu \cdot t) \tag{8b}$$

Transfer processes in the reactor

The most significant reactor properties relate to the input of energy, oxygen, and heat, and to heat removal and mixing. They are generally described by experimental terms linking different dimensionless values together. These latter are derived from either similarity theory taking fundamental equations for physical processes as a basis, or are determined by dimensional analysis of possible variables. In particular, dimensionless groups for hydrodynamic processes are derived from the Navier-Stokes differential equations.

2.3.1 Power input in cultivation media

2.3.1.1 Stirred tank reactor

In nonaerated liquids the impeller power input P_R $\left(W = \frac{kg \cdot m^2}{s^3} = \frac{J}{s}\right)$ is generally based on the impeller speed N_R (1/s) and diameter d_R (m), and of the kinematic viscosity ν (m^2/s). Dimensional analysis yields the following dimensionless values:

$$Ne_R = \frac{P_R}{N_R^3 d_R^5} \text{ Newton number and}$$

$$Re_R = \frac{N_R d_R^2}{\nu} \text{ Reynolds number}$$

The impeller power input in a stirred tank in generally based on equations for Ne_R and Re_R in nonaerated liquids:

$$Ne_R = k_1 \frac{1}{Re_R} \quad (11a)$$

$$P_R = k_2 N_R^2 d_R^3 \eta \quad (12a)$$

for laminar flow ($Re_R < 10$) in baffled systems (reactors with in-built guiding plates), whereas for turbulent conditions this changes to

$$Ne_R = k_2 \quad (11b)$$

$$P_R = k_2 N_R^3 d_R^5 \rho \text{ for } Re_R > 10^2 \quad (12b$$

For low-viscous turbulent liquids the Ne_R values vary over a broad range: $Ne_R \approx 5$ (flat bladed disc turbine (6 blades)), 0.65 (MIG impeller) at $Re_R = 10^5$. For Ne_R in the intermediate region ($10 < Re_R < 10^2$) the following relationship was obtained:

$$Ne_R = k_3 \ Re_R^{-1/3} \quad (11c)$$

In these relationships k_1, k_2, k_3 are constants. For non-Newtonian liquids an effective viscosity η_e is used:

$$\eta_e = \frac{\tau}{\left(\frac{du}{dx}\right)} \quad (13)$$

in which τ is the shear stress (kg/m s^2) and $\left(\frac{du}{dx}\right)$ is the mean shear gradient (1/s).

According to Metzner and Otto [6]

$$\left(\frac{du}{dx}\right) = k^* N_R \text{ with } k^* \approx 10 - 12 \quad (14)$$

For non-Newtonian nonaerated liquids the constants k_1 and k_2 are in the following range: $k_1 \approx 75$ (for flat bladed disc turbine) and 50–68 (for various MIG impellers); $k_2 \approx 0.5$ (for flat bladed disc turbine) and 0.5 (for various MIG impellers). For gas-stirred reactors Ne_R is often given as a function of the aeration group Q_G. This is the aeration rate q_G (m^3/s) with respect to the amount of the liquid passing radially through the stirrer (pump capacity):

$$q_G = Q_G N_R d_R^3 \ Q_G \text{ is dimensionless: } Q_G = \frac{q_G}{N_R d_R^3} \quad (15)$$

Hughmark [7] recommended the following relationship for the ratio of power input in aerated P_G and nonaerated P_R reactors with flat bladed disc turbines:

$$\frac{P_G}{P_R} = C_2 \left(\frac{N_R^2 d_R^4}{g B V_L^{2/3}}\right)^m \left(\frac{q_G}{N_R V_L}\right)^n \quad (16)$$

in which B is the blade width, $C_2 = 0.10$, $m = -0.20$, $n = -0.25$. This relationship was reconfirmed by several authors.

Tower reactor

In a tower reactor (without stirrer), in which gas compression is the only source of energy, the power input P_B can be determined as follows:

$$P_G = M_G \left[RT \ \ln\left(\frac{P_{in}}{P_{out}}\right) - gH - \frac{1}{2}\left(w_{Gout}^2 - w_{Gin}^2\right)\right] \quad (17)$$

in which M_G (kg/s) is the gas mass flow, R (m^2/s^{2}K) is the gas constant, P_{in}, P_{out} (Pa) is the gas pressure at column inlet and outlet, H (m) is the height of the aerated column, w_{Gin} and w_{Gout} (m/s) is the effective gas velocity at column inlet and outlet and g (m/s^2) is the acceleration of gravity. The gas throughput $\frac{q_G}{V_L}$ (1/s) which is a function of the liquid volume V_L, and the superficial gas velocity based on the cross-sectional area of the column A (m^2) $\frac{q_G}{A} = w_{SG}$ (m/s), are used to define the aeration rate of the reactor.

Oxygen transfer into the cultivation media

The volumetric mass transfer coefficient k_La (Table 2) can be derived from the oxygen transfer rate (OTR) Q_G:

$$k_L a = \frac{Q_{O_2}}{O_F^* - O_{F1}}$$

in which Q_{O_2} (kg/m^{3}s) is the oxygen transfer rate based on the liquid volume.

Table 2. Volumetric mass transfer coefficients k_La in CMC solutions in a bubble column with a diameter of 14 cm, a height of 400 cm, and porous plat gas distributor at about the same specific power input P_B/V_L

CMC (%)	P_B/V_L (kW · m^{-3})	$k_La\ 10^2$ (s^{-1})
1.0	0.525	4.9
1.2	0.545	4.1
1.4	0.525	3.0
1.56	0.525	3.0
1.7	0.550	2.0

O_F^* (kg/m^3) is the dissolved oxygen concentration at the gas/liquid interface, O_{F1} (kg/m^3) is the dissolved oxygen concentration in the bulk liquid, k_L (m/s) is the mass transfer coefficient through the gas/liquid interface, and a (1/m) is the specific gas liquid interfacial area based on the liquid volume.

$$a = \frac{a^*}{V_L} = \frac{6\varepsilon_G}{d_S(1 - \varepsilon_G)}$$

in which a^* is the gas liquid interfacial area and ε_G is the gas hold up.

$$\varepsilon_G = \frac{V - V_L}{V}$$

in which V is aerated liquid volume, V_L is the nonaerated liquid volume

d_S is the Sauter bubble diameter:

$$\frac{d_S = \sum n_i d_i^3}{\sum n_i d_i^2}$$

in which n_i is the frequency of bubbles with diameter d_i.

For coalescing liquids a dimensionless relationship was recommended [8]:

$$k_L a \left(\frac{q_G}{V_L}\right)^{-1} = 1.5 \times 10^{-2} \left(\frac{P_G}{q_G}\right)^{*0.5} \quad (18)$$

$$\text{with} \left(\frac{P_G}{q_G}\right)^{*} = \frac{\left(\frac{P_G}{q_G}\right)}{(g\,\nu)^{2/3}\rho_L} \quad (19)$$

For noncoalescing liquids a similar relationship was recommended:

$$(k_L a)^{*} = 1.1 \times 10^{-4} \left(\frac{P_G}{V_L}\right)^{*} \quad (20)$$

$$\text{with } (k_L a)^{*} = (k_L a)\left(\frac{\nu}{g^2}\right)^{1/3} \quad (21a)$$

$$\text{and } \left(\frac{P_G}{V_L}\right)^{*} = \left(\frac{P_G}{V_L}\right)\left[\rho_L (\nu g^4)^{1/3}\right]^{-1} \quad (21b)$$

in which ν is the kinematic viscosity and ρ_L the density of the liquid.

Heat balance in the reactor

The heat balance of the reactor consists of following heat sources:

$$R_{Tot} = R_{Diss} + R_{Flow} + R_{Met} + R_{Vap} + R_{Trans}(W) \quad (22)$$

R_{Tot} is the total heat generated (W), R_{Diss} is the heat dissipated by stirrer and mechanical foam destroyer (W), R_{Flow} is the heat generated by the flowing gas (W), R_{Met} is the heat generated by the metabolic activity of the microorganisms (W), R_{Vap} is the heat loss by vaporization (W), and R_{Trans} is the heat loss through the reactor wall (W).

The heat generated by the metabolic activity of the microorganisms can be determined from the oxygen balance for aerobic cultivation according to

$$R_{Met} = -460 \times 10^3 R_O(W) \quad (23a)$$

$$R_{Met} = 460 \times 10^3 \times OUR \times V_B \quad (23b)$$

where OUR is the oxygen uptake rate and V_B is the volume of the medium.

For anaerobic growth the developed heat is related to the C-consumption rate. The heat dissipated by stirrer and antifoam destroyer is given by the power input into the reactor P_R, which depends on stirrer type and speed, reactor construction, and medium viscosity. The heat generated by the compression of the gas is about the same which occurs during isothermal decompression; thus, the net effect is zero. The heat loss resulting from vaporization depends on the aeration rate temperature of the reactor and vapour composition:

$$R_{Vap} = -C_{vap} F_G \left(\frac{P_{in}}{P_{out}} \rho_{vapo} - \rho_{vapt}\right)(W) \quad (24)$$

in which C_{vap} is the heat of vaporization (J/kg°C), P_{in}, P_{out} are the pressure at bottom and at the top of the cultivation medium (N/m^2), ρ_{vapo} is the vapor concentration in the air at the temperature of the medium, and top pressure ρ_{vapt} is the vapor concentration of the inflowing air (kg/m^3).

The heat loss through the reactor wall depends on reactor isolation and cooling rate:

$$R_{Trans} = k_W A_{Col}(T_R - T_C)(W) \quad (25)$$

in which k_W is the overall heat transfer coefficient from medium to cooling liquid (W/m^2 °C), A_{Col} is the surface area of the heat exchanger (cooler) (m^2), and T_R, T_C are the temperatures of the cultivation medium and the cooling liquid (°C).

$$\frac{1}{k_W} = \frac{1}{\alpha_1} + \frac{d_l}{\lambda_1} + \frac{d_W}{\lambda_W} + \frac{1}{\alpha_2} \quad (26)$$

in which α_l is the heat transfer coefficient of the cultivation medium (W/m^2 °C,), α_2 is the heat transfer coefficient of the cooling medium (W/m^2 °C), d_l is the thickness of the fouling layer (m), d_W is the wall thickness of the cooling coil (m), λ_l is the heat conductivity of the fouling layer (W/m °C), and λ_W is the heat conductivity of the cooling wall (W/m °C).

According to Henzler [9] the heat transfer coefficient for the cultivation medium in a stirred tank (Table 3) is given by

$$\frac{\alpha_1 D_R}{\lambda_m} = 0.6\left(\frac{N_R d_R^2}{\nu_m}\right)^{0.67}\left(\frac{C_{pm}\eta_m}{\lambda_m}\right) \quad (27)$$

in which λ_m is the heat conductivity of the cultivation medium (W/m °C), D_R is the diameter of the reactor (m), ν_m is the kinematic viscosity of the cultivation medium (m^2/s), C_{pm} is the thermal coefficient of the the cultivation medium (J/kg °C), and η_m is the dynamic viscosity of the cultivation medium (N s/m^2).

In bubble column the heat transfer coefficient of the cultivation medium is given according to Heinen and van't Riet [10]:

Table 3. Heat transfer coefficient as a function of the specific power input (P_G/V_L) in a stirred tank (D_R = 40 cm, H = 40 cm) with 0.5% CMC solution and flat-bladed disc turbine SB (d_R/D_R = 0.33) and 2 stirrers, SB and IMIG (d_R/D_R = 0.60).

	P_G/V_L (kWm^3)	α_1 (Wm^{-2}K^{-1}
SB	10^{-1}	4×10^2
	10^0	1×10^3
	10^1	2.5×10^3
IMIG	10^{-1}	1×10^3
	10^0	2.5×10^3
	10^1	4×10^3

$$\alpha_1 = 9391(w_{SG})^{0.25}\left(\frac{\eta_W}{\eta_m}\right)^{0.35} \quad (28)$$

in which w_{SG} is the superficial gas velocity (m/s) and η_W is the dynamic viscosity of water (N s/m^2).

If all heat flows entering or leaving the bioreactor are identified, calorimetric instrumentation enables on-line dynamic heat balance estimations. Calculation of the heat released or taken up during an operational bioprocess was shown to constitute a cost-effective approach for the development of production processes [11].

3 Scale-up of 4-decanolide production

The microbial reduction and cyclization of 4- and 5-oxo-octanoic to dodecanoic acids yields a series of optically pure alkanolides that impart various powerful fruity, nutty, and fatty odor attributes to food. After (4*R*)-(+)-decanolide, obtained from the conversion of 12-hydroxy oleic acid, a genuine constituent of castor oil, entered the market at initial prices of up to 20 000 US$ kg^{-1}, every major flavor company has patented and up-scaled respective bioprocesses. Most of these bioprocesses were based on yeasts or on deuteromycetes.

The studies on fungal formation of 4-decanolide presented here as a case study started with the observation that a plate culture of the basidiomycete *Tyromyces sambuceus*, when grown on one of the screened nutrient media, exhibited a pleasant exotic odor reminding of passion fruit and peach. Only trace concentrations of (4*R*)-(+)-decanolide (<5 μg · L^{-1}) were detected by capillary gas chromatography-mass spectrometry in cultures that were grown over a period of four to six weeks. The cells were transferred to shake flasks, and a systematic improvement of the nutrient medium based on statistically backed experimental design [12] was conducted. A low productivity of 7 μg · L^{-1}d^{-1} was received in synthetic minimal medium (Fig. 1). Further process development (Fig. 1, steps 2 and 3) comprised the use of different C-sources, such as peanut oil or sunflower oil, to stimulate the acyl metabolism of the mycelial cells.

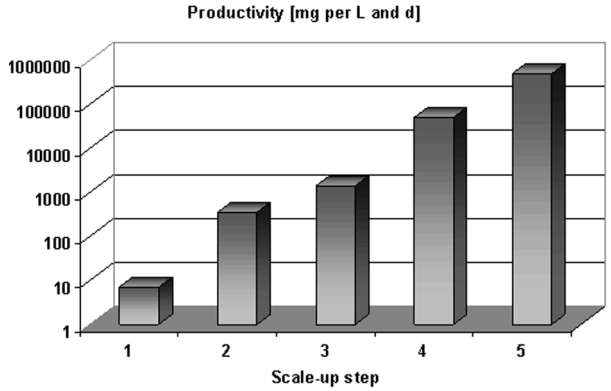

Figure 1. Scale-up of a pellet culture of the basidiomycete *Tyromyces sambuceus* generating (4*R*)-(+)-decanolide.

While some significant effects were recorded, only the supplementation of castor oil resulted in a breakthrough (Fig. 1, step 4). Obviously, the introduction of the oxygen atom into the chain of the fatty acid presented the rate-limiting metabolic step.

In terms of productivity, a pellet inoculated laboratory-scale stirred tank reactor was superior over the filamentous form of the (homogenized) inoculum. Improved mechanical stability and the natural way of immobilization may have accounted for this finding. At the same time, viscosity was apparently reduced. This in turn reduced the power requirements according to Section 2.3.1.1 and the transfer of heat according to Henzler's equation (*cf.* Section 2.3.3). The example shows that the separate consideration of physiological and physical parameters during scaling-up is not possible. It is also evident that changes of the cell morphology or other biological parameters which cannot be easily computer-predicted may have a considerable impact on the overall process.

Although formation of 4-decanolide from added castor oil by *T. sambuceus* was a rapid process, oxygen transfer (*cf.* Section 2.3.2) was not a limiting factor in these slowly growing fungal cultures. The calculation of the carbon balance of bioreactor grown cells according to Section 2.1 combined with the monitoring of growth (*cf.* Section 2.2.1) showed that most of the triacyl glycerol substrate added was catabolized and converted to biomass and carbon dioxide. Therefore, subsequent steps focused on establishing a semi-continuous process in a 15 L reactor (Infors ISF-200) to evaluate parameters that would help to direct the fungal metabolism towards accumulation of (4*R*)-(+)-decanolide and its immediate hydroxy acid precursor. Removal of spent nutrient medium and cell recycle was performed using a tubular off-line filtration unit (Fig. 2). A complete uncoupling of growth and 4-decanolide formation was not

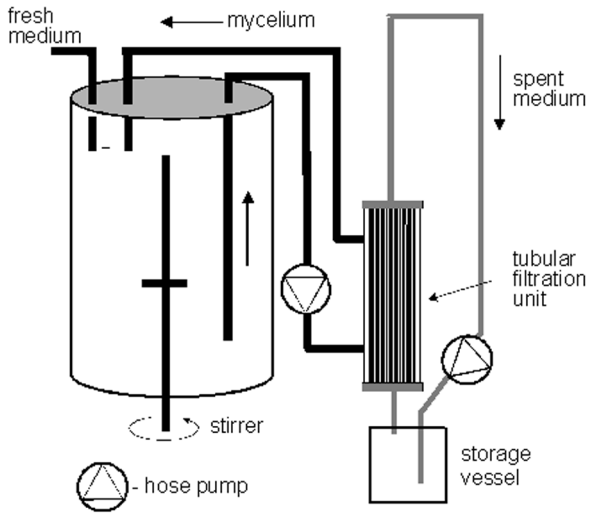

Figure 2. Stirred tank cultivation coupled with cross-flow filtration according to Fig. 1, step 5.

achieved, but high peak productivities were still recorded upon application of a fed-batch feeding regime of the precursor fatty acid (Fig. 1, step 5). The problem of excessive foaming, caused by the intermediary di- and mono-acylglycerols, was solved by controlled slow addition of the lipid substrate. Silylated glass surfaces and electro-polished steel surfaces reduced fouling effects that constitute one of the major problems in up-scaling of basidiomycete cultures.

Bioprocesses for the generation of volatile lactones have paved the way to today's advanced biotechnology of flavors, and quite a number of alkanolides (and other volatile flavors) are successfully manufactured on the 50–500 L scale. Some typical target compounds of aroma biotechnology are highly potent, and larger-scale operations are, thus, sometimes not required, because an annual production of some hundred grams of product may be sufficient to meet the market demands. Conventional batch processes and extraction or distillation dominate the industrial applications, partly because of ease of operation, partly because of reluctance to introduce novel processing strategies. Membrane- or adsorbent-based downstreaming steps are often superior to the classical processes, preferably if the cold recovery of sensitive fine chemicals is intended [13–16].

The on-line monitoring of waste gas volatiles beyond carbon dioxide and oxygen (*cf.* Section 2.1) is a typical field of application of electronic noses. When a recombinant animal (CHO) cell line was used to produce human blood coagulation factor VIII, cellular state transitions and changes related to product formation were successfully followed [17]. Microbial infections, particularly critical on the production scale, were also detected at an early stage. The production of avermectins by *Streptomyces avermitilis* was proportional to the intensity of a fermentation odour identified as geosmin (earthy, beet-root odor) [18]. The scale-up of such a bioprocess could also benefit from an on-line control of the concentration of the volatile emanations.

4 Scale-up of the downstreaming step

The principles of the scale-up of the downstreaming of high-molecular products from biotechnological processes will be demonstrated for a high-value protein from milk. Milk is a highly complex mixture of various compounds, and downstreaming is extremely difficult. Here lactoferrin is treated as a high-value product from regular milk [19].

Lactoferrin is a multifunctional iron-binding glycoprotein found in external secretions, milk, saliva, tears, and other sources. Its molecular mass is 77 kDa, and it contains two binding sites for Fe^{3+}. This capacity to bind iron partly explains lactoferrin's antibacterial and antifungal activities. Other bioactivities, such as an effect on cell growth, its immuno-stimulating action, and even anti-human immunodeficiency virus (HIV) activity have been demonstrated [20–22]. Some internet suppliers associate the protein with less proven health claims.

Conventional chromatographic processes show tremendous disadvantages for a fast and reliable downstreaming of whey, since large volumes and high protein concentrations cause many problems, such as fouling of chromatographic material, long cycle times, large pressure drops *via* chromatographic columns, and complicated process control systems. A newly developed membrane adsorber technology offers the possibility to recover high value proteins from whey *via* adsorber filtration processes. Filtration is a well-accepted and well-studied unit operation in dairy technology, and scaling-up on the basis of general scale up rules is well understood (*cf.* Section 5). Membrane adsorber technology combines chromatographic separation with filtration. The interactions between dissolved molecules and the functional groups on the membranes inner surface occur in convective through-pores rather than in stagnant fluid inside the pores of an adsorbent particle. Therefore, the loading and elution of membrane adsorbers can be performed at high fluxes resulting in short cycle times with sharp breakthrough curves. Channeling cannot occur, scale-up is easy, and materials and systems allow cleaning in place (CIP) procedures.

As shown in Fig. 3, membranes can be converted into efficient and selective adsorbers by attaching functional exchanger groups to the inner surface of the microporous membranes. That means that the pores of the membranes are covered with the functional groups. Depending on the

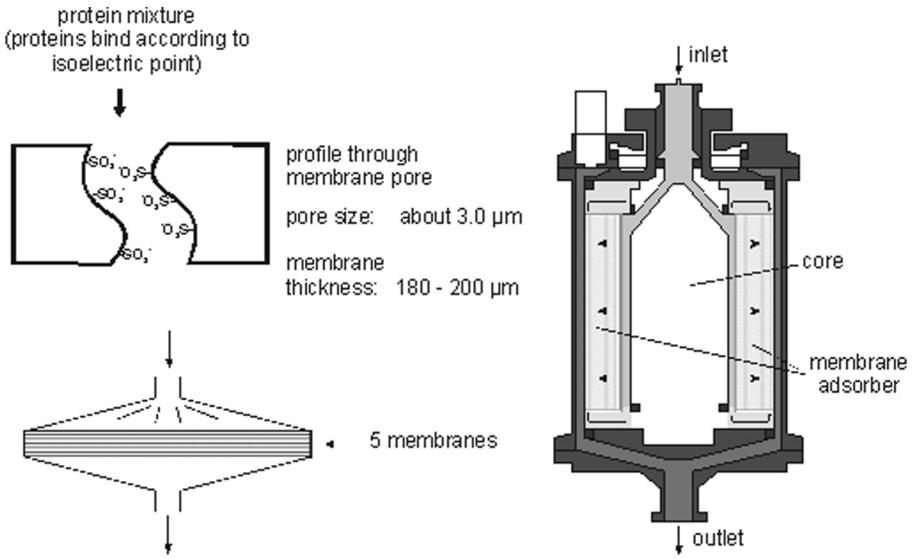

Figure 3. Principle of membrane adsorber technology. A capsule with 10–100 cm^2 membrane area and a spiral module with a membrane area of up to 8 m^2 are shown.

choice of the functional group various adsorber systems can be obtained, such as ion exchanger, affinity or metal affinity adsorber systems. Commercially available membrane systems for laboratory and process scales are ion exchanger systems with strongly acidic (sulfonic acid), strongly basic (quarternary ammonium), weakly acidic (carboxylic acid), and weakly basic (diethyl amine) types.

Ion exchanger membrane systems are available in small modules with 10 to 100 cm^2 of membrane surface (one up to ten layers) or in spiral bound systems as shown in Fig. 3. The spiral modules offer the possibility of a large surface area in small capsules (1 – 8 m^2). The modules can be operated in parallel or in a series. In these modules, the membrane adsorber is rolled up to form a binding bed. The feed enters the module from the top and is distributed by the center dead volume-reducing unit to the internal membrane channel, passing the membrane in an orthogonal flow. The eluate is collected in an extra external channel and guided to the outlet. The formal kinetics of these modules can be easily understood and modelled based on the material balances as mentioned in Section 2. Here the modules can be regarded in batch or continuous mode.

For preliminary experiments, strongly acidic membranes in flat-sheet polysulfonate modules (Sartobind S 15, Sartorius, Göttingen, Germany) membrane layers of 15 cm^2 total adsorber area) were used. These modules can be integrated in fast protein liquid chromatography systems (*e.g.*, Bio-Rad, Munich, Germany) equipped with a UV detector and electric conductivity measurement for monitoring the isolation process [23]. The flow can be adjusted from three to 50 mL/min. This setup offers the possibility to run repeated cycles of loading and elution of lactoferrin under different conditions. The pH flow rate and the elution buffer composition were optimized. The maximal dynamic loading capacity was found to be 0.2 mg · cm^{-2} membrane material (pH of whey was 6.2) and best elution was obtained with 1 mol sodium chloride solution. Up to 50 loading and elution profiles could be run without any loss of sensitivity and at constant flow rate in the system. From these experiments, which were verified with microfiltrated whey samples, a direct scale-up from 15 cm^2 to 4 m^2 was performed.

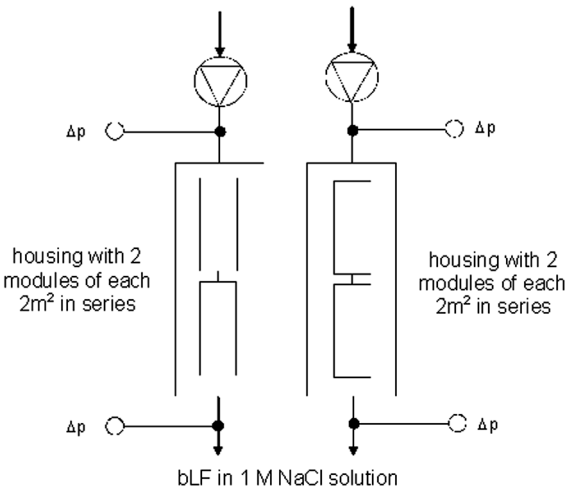

Figure 4. Setup for the twin system with two 2×2 m^2 modules (bLF: bovine lactoferrin).

Figure 4 shows a principle setup of a twin membrane adsorber unit with 4 m^2 modules (Sartobind factor-two family; Sartorius). The loading and elution profiles were monitored *via* UV spectrometry, electric conductivity, and flow volume monitoring. The whole twin unit was operated *via* a computer system for repeated loading and elution. Up to

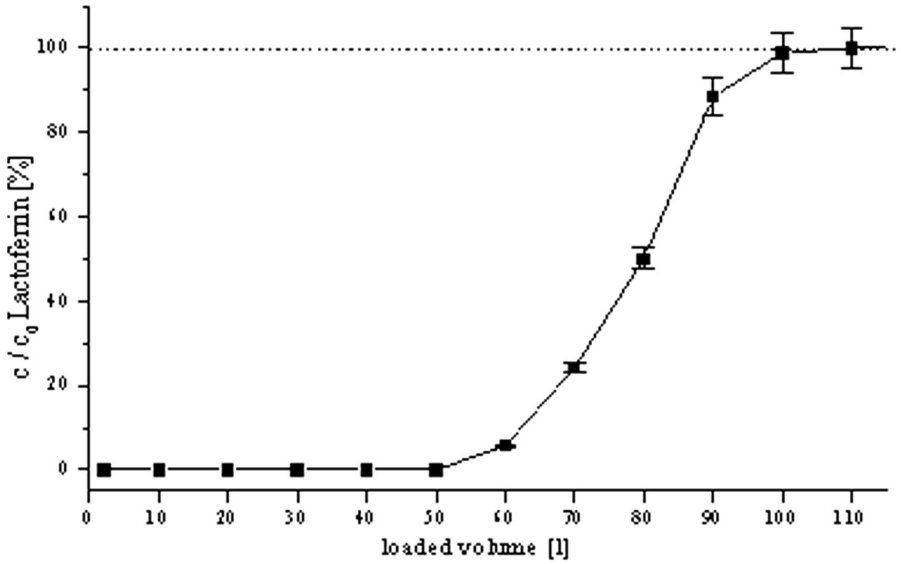

Figure 5. Breakthrough behavior of the $2 \times 2 m^2$ modules.

105 L whey from the microfiltration unit were directly pumped into the first membrane adsorber unit with a flow rate of 8 L · min^{-1} (inlet pressure two bar). Figure 5 shows the breakthrough curve monitored *via* the UV-monitor. After 105 L the breakthrough was 100%. Afterwards the system was washed with 8 L buffer (20 mmol sodium phosphate buffer, pH 6.2), in order to wash out unbound proteins and to reduce the UV-signals. A stepwise increase of elution buffer to 1 mol sodium chloride solution resulted in a direct elution of the bound lactoferrin. Within 120 min one complete loading and elution cycle was performed. Afterwards a short regeneration cycle with 10 L buffer was necessary prior to the next loading and elution cycle. The balances of the loading/elution cycles can be performed according to the model equations mentioned in Sections 2.1 and 2.3, without using the terms of cell growth.

The loading capacity of a 4 m^2 module was in the range of 8 g per loading (dynamic capacity 0.2 mg · cm^{-2}). The analysis of the elution fraction indicated a lactoferrin concentration of 7.76 g of lactoferrin which is nearly 97% of the theoretical value. Regarding the error range of a regular HPLC analysis, the results of the maximum dynamic capacity and the 15 cm^2 modules could be verified in the 4 m^2 module. The easy scale-up from the miniaturized modules to the production plant modules becomes obvious by these results. A direct transfer of the lab experiments into a large scale unit is possible simply using similarity comparison (*cf.* Section 5, [24]).

In repeated loading elution experiments, 1000 L of microfiltrated whey permeate was loaded in ten cycles to the membrane adsorber modules and eluted afterwards. In contrast to the laboratory experiments mentioned above, a slight decrease in the flow rate (loading) was observed and the back pressure in the system was increasing. The whole cycle time increased from about 15 min to 2 h, and the lactoferrin recovery decreased by nearly 20%. Within the first four cycles the lactoferrin recovery was above 88%, and a membrane cleaning was necessary after four cycles under the tested conditions (cleaning temperature 40°C; cleaning cycle acids, 10 min, two separated cleaning steps, 10 min). The whole regeneration and cleaning cycle took 45 min. The results of these up-scale experiments indicate that microfiltrated whey solution can be directly downstreamed *via* membrane adsorber systems. The dynamic binding capacity for lactoferrin was 0.2 mg · cm^{-2}. Up to four cycles can be run with the 4 m^2 module in series, afterwards a cleaning step is necessary to completely regenerate the module.

For continuous processing the twin column system (Fig. 4) must be operated in the following way: while one module is loaded, the other module is eluted. The following assumptions and calculations can be made: In a production plant, the inlet pressure would be increase to 7 bar (flow: 24.5 L · min^{-1}) and the recovery of lactoferrin would be for four cycles (88% each). Based on the results of the pilot plant lab experiments 4 h per day would be necessary for cleaning, while 20 h could be covered by loading elution cycles. Energy input and chemical usage (also necessary for environment purposes) are necessary to regard to get a rough economic estimation. The following results can be obtained for such twin plant systems:

Loading flux:	24.5 L · min^{-1} (pin = 7 bar)
Cycle time:	3.5 min (loading per module)
Lactoferrin (bLF) yield per cycle:	7 g bLF (88% maximum yield)
Lactoferrin (bLF) yield per day:	2380 g bLF
Lactoferrin (bLF) per year:	714 kg bLF (300 days)

In order to increase the capacity to downstream 100 000 tons of whey per year, a production plant with 80 m^2 adsor-

ber area would be necessary in a twin plant setup, and 7140 kg bLF could be downstreamed.

The costs would be the following:

Fixed:	– depreciation (10% linear over 10 years)	51 000 EUR
	– interest on borrowed money	15 000 EUR
	– maintenance	10 500 EUR
	Σ	77 000 EUR
Variable:	– modules (80 m^2, list price)	250 000 EUR
	– chemicals (NaCl, buffer)	175 000 EUR
	– energy (18 000 kW)	2 500 EUR
	– cleaning agents (NaOH, citric acid)	76 500 EUR
	– H_2O (6.5 EUR m^{-3} incl. wastewater)	77 000 EUR
	– manpower	76 500 EUR
	Σ	612 500 EUR
fix costs + variable costs:		689 500 EUR
cost per unit:		96.5 EUR/kg bLF

Supplementary costs:
– crossflow microfiltration
– desalting/concentrating
– spray drying

These calculations show that the large-scale production of lactoferrin from whey would be possible in a twin plant system. The dimension and throughput was calculated from lab and pilot plant data. The production of lactoferrin would cost about 96.5 EUR kg^{-1}. These costs could easily be reduced by re-using the elution solutions. Lab experiments showed that the elution buffer could be used four times without any loss of efficiency. In addition, the module costs would decrease, if larger amounts would be produced for large-scale production units.

Table 4. Balance of chemicals needed to run the twin unit

	H_2O	NaCl	NaH_2PO_4	Na_2HPO_4
1 cycle (3.5 min)	32 L	490 g	50 g	57.5 g
h	410 L	4.17 kg	638 g	750 g
Day	8.2 t	83.5 kg	13 kg	15 kg
Year	2460 t	25 t	3.9 t	4.5 t

5 Scale-up rules

It is assumed that the metabolism of a microorganism is not influenced by the size of an ideal reactor. Only the transfer processes vary with the reactor size. During scale-up the reactor volume increases. The heat removal rate R_{Total} from the reactor is affected most, because the volume changes with third power of the linear scale, and the heat exchanger surface with the second power only. Because of the increased volume of the cultivation medium the homogeneous distribution of substrates and dissolved oxygen becomes more and more difficult. These problems become more serious in highly viscous media, as, for example, with higher fungi (*cf.* Section 3), and with high cell density cultivations.

For scale-up process several recommendations were made:

If the model reactor is labeled with index 1 and the full-scale one with 2, the reactors 1 and 2 should have: (i) equal mixing time; (ii) equal mass transfer coefficient (*cf.* Section 2.2.1); (iii) equal tip speed of the stirrer blade (>5 to 7 $m \cdot s^{-1}$ shear rate may become critical; larger cells or cells without a rigid cell wall, such as animal cells, are more sensitive to shear stress (*cf.* Section 2.3.1.1) [25]); (iv) equal dissolved oxygen concentration (*cf.* Section 2.2.1); (v) equal cooling rate R_{Total} with respect to the medium volume V_L (*cf.* Section 2.3.3).

The total heat generated R_{Tot} is predominantly influenced by the heat dissipated by the impellers R_{Diss} in stirred tank reactors. Therefore, the power input P_R is the most important parameter. The maximum value of P_R/V_L is limited by the maximum possible cooling rate R_{Trans} in stirred tank reactors. According to this rule, the power input per liquid volume of model 1 and full-scale 2 should be equal.

In tower reactors (*cf.* Section 2.3.1.2) P_G/V_L is not limited by the cooling rate, because the power input is maintained merely by aeration, and the heat produced is removed by decompression of air along the column. By assuming geometrical similarity of these reactors, the following rule can be applied [26]:

$$\frac{\left(\frac{P_R}{V_L}\right)_2}{\left(\frac{P_R}{V_L}\right)_1} = f\left(\frac{d_{R2}}{d_{R1}}\right) = \left(\frac{d_{R2}}{d_{R1}}\right)^y \tag{34}$$

or

$$\frac{\left(\frac{P_R}{V_L}\right)_2}{\left(\frac{P_R}{V_L}\right)_1} = f\left(\frac{V_2}{V_1}\right) = \left(\frac{V_2}{V_1}\right)^{y/3} \tag{35}$$

in which d_{R1} and d_{R2} are the impeller diameters in reactors 1 and 2.

The most common scale-up rule is constant power input per unit volume in model reactor 1 and full-scale reactor 2.

There are some other (qualitative) rules for scale-up [26]:

$$\left(\frac{P_{R2}}{P_{R1}}\right) = \left(\frac{V_{L2}}{V_{L1}}\right)^{S+1} \tag{36}$$

The magnitude of *s* depends on the scale-up strategy:

Scale up strategy	s
Maintain k_La and w_{sG} constant	0.16
Maintain P/V constant	1.0
Maintain $\pi d_R N_R$ constant (for turbulent mixing)	–1/3
Maintain $\pi d_R N_R$ constant (for laminar mixing in highly viscous medium)	–2/3
Maintain Re_R constant	–4/3

The transfer processes as a function of the power input and other parameters are evaluated in laboratory and pilot plant systems. By means of the similarity theory it is possible to transfer these results, if they are applied in dimensionless equations, to full-scale equipment.

6 Practical problems with the similarity theory and scale up rules

Sound relations between apparatus and process parameters have to be ascertained for a successful scale-up. Because of the complexity of the real systems drastic simplification of the model and of full-scale reactors and processes is necessary. The model and the full-scale reactors are not ideally mixed. Considerable heterogeneity prevails in the cultivation medium of full-scale reactors. This causes local and temporal variations of the concentrations of dissolved oxygen and substrates as well as the temperature and the pH-value, which influence the metabolism of the microorganism. It has, for example, been impossible to synchronize a fed-batch culture of *Saccharomyces cerevisiae* due to the unavoidable glucose gradients in the stirred tank reactor [27]. The transfer rates are functions of the scale-up. These influence the metabolism of the microorganism as well. Most of the key parameters (concentrations of microorganism, substrate, oxygen uptake rate, viscosity of the medium) vary considerably during the cultivation. For the calculations of transfer parameters space and time average values are used, which can cause serious errors.

It is impossible to meet the geometric, fluid dynamic, mass transfer, heat transfer, and kinetic similarity of the model and full-scale reactors at the same time. Looking at the geometrical similarity of model and full-scale reactor this requirement is not fulfilled, because the reactor height to diameter ratio is considerable larger in full-scale than in the model reactor. The transfer of results obtained on the idealized model to the idealized full-scale reactor is therefore bound to be inaccurate. To reduce the increasing scale-up errors with enlargement of the volume ratio of reactors, a multistage scale-up approach with a scale-up factor of 10 for each stage for the coupling kinetic, hydrodynamic, and transport processes in bioreactors is recommended.

Up-scaling considerations should not be restricted to the bioreactor itself, but should include the entire process in an integrated view. Modern software allows to run bioprocess simulations on the computer; some of them incorporate downstreaming operations, such as ion or affinity chromatography and the related cost calculations [28]. The above complications, however, usually prevent a scale-up based exclusively on a computer. Experimental investigations across the increasing scales are necessary.

7 References

[1] Asaff-Torres, A., De la Torre-Martinez, M., Bioprocess design. In: Gutierrez-Lopez, G. F., Barbosa-Canovas, G. V., (Eds.), *Food Sci. Food Biotechnol.* 2003, 81–104.

[2] Berger, R. G., *Aroma Biotechnology*, Springer, Heidelberg, Berlin 1995.

[3] Stentelaire, Ch., Lesage-Meessen, L., Oddou, J., Bernard, O., *et al.*, Design of a fungal bioprocess for vanillin production from vanillic acid at scalable level by *Pycnoporus cinnabarinus. J. Biosci. Bioeng.* 2000, *89*, 223–230.

[4] Bonham-Carter, J., Ives, P., Reeks, D., Real-time off-gas analysis improves bioreactor efficiency. *BioProcess Int.* 2004, *2*, 76–79.

[5] Roels, J. A., Application of macroscopic principles to microbial metabolism. *Biotechnol. Bioeng.* 1980, *22*, 2457–2514; Heijnen, J. J., Roels, J. A., A macroscopic model describing yield and maintenance relationships in aerobic fermentation processes. *Biotechnol. Bioeng.* 1981, *23*, 739–763.

[6] Metzner, A. B., Otto, R. E., Agitation of non-Newtonian fluids. *AIChE J.* 1957, *3*, 3–10.

[7] Hughmark, G. A., Power requirements and interfacial area in gas-liquid turbine agitated systems. *Ind. Eng. Chem. Process Design Dev.* 1980, *19*, 638–641.

[8] Zlokarnik, M., Sorption characteristics for gas-liquid contacting in mixing vessels. *Adv. Biochem. Eng*. 1978, *8*, 133–151.

[9] Henzler, H. J., Engineering design data for stirred vessels as fermentors. *Chem. Ing. Techn*. 1982, *54*, 461–462, 465–472, 475–476.

[10] Heijnen, J. J., Van't Riet, K., Mass transfer, mixing and heat transfer phenomena in low viscosity bubble column reactors. *Chem. Eng. J.* 1984, *28*, B21–B42.

[11] Voisard, D., Pugeaud, P., Kumar, A. R., Jenny, K., *et al.*, Development of a large-scale biocalorimeter to monitor and control bioprocesses. *Biotechnol. Bioeng.* 2002, *80*, 125–138.

[12] Böker, A., Fischer, M., Berger, R. G., Raspberry ketone from submerged cultured cells of the basidiomycete *Nidula niveotomentosa. Biotechnol. Prog*. 2001, *17*, 568–572.

[13] Dufosse, L., Blin-Perrin, C., Souchon, I., Feron, G., Microbial production of flavors for the food industry. A case study on the production of gamma-decalactone, the key compound of peach flavor, by the yeasts *Sporidiobolus* sp. *Food Sci. Biotechnol*. 2002, *11*, 192–202.

[14] Stark, D., Münch, Th., Sonnleitner, B., Marison, I. W., von Stockar, U., Comparison of different *in situ* product-removal methods to enhance the production of the aroma compound 2-phenylethanol. Abstracts, *219th ACS National Meeting*, San Francisco, CA 2000.

[15] Etschmann, M. M. W., Bluemke, W., Sell, D., Schrader, J., Biotechnological production of 2-phenylethanol. *Appl. Microbiol. Biotechnol*. 2002, *59*, 1–8.

[16] Gehrke, M., Krings, U., Berger, R. G., Selective recovery of flavour compounds using reversed phase polystyrene adsorbents. *Flav. Fragr. J.* 2000, *15*, 108 – 114.

[17] Bachinger, T., Riese, U., Eriksson, R., Mandenius, C.-F., Monitoring cellular state transitions in a production-scale CHO-cell process using an electronic nose. *J. Biotechnol.* 1999, *76*, 61 – 71.

[18] Rezanka, T., Votruba, J., Fermentation odor and bioprocess scale-up. *Bioproc. Engin.* 1998, *19*, 159 – 160.

[19] Masson, P. L., Heremans, J. F., Lactoferrin in milk from different species. *Comp. Biochem. Physiol.* 1971, *39B*, 119 – 129.

[20] Sanchez, L., Calvo, M., Brock, J. H., Biological role of lactoferrin. *Arch. Dis. Childh*. 1992, *67*, 657 – 661.

[21] Harmsen, M. C., Swart, P. J., de Bethune, M. P., Pauwels, R., *et al.*, Antiviral effects of plasma and milk proteins: lactoferrin shows potent activity against both human immunodeficiency virus and human cytomegalovirus *in vitro. J. Infect. Dis.* 1995, *172*, 380 – 388.

[22] Lampreave, F., Pineiro, A., Brock, J. H., Castillo, H., *et al.*, Interactions of bovine lactoferrin with other proteins of milk whey. *Int. J. Biol. Macromol.* 1990, *12*, 2 – 5.

[23] Riechel, P., Weiss, T., Weiss, M., Ulber, R., *et al.*, Analysis of bovine lactoferrin in whey using capillary electrophoresis and micellar electrokinetic chromatography. *J. Chromatogr. A* 1998, *817*, 187 – 193.

[24] Demmer, W., Nussbauer, D., Large-scale membrane adsorbers. *J. Chromatogr. A* 1999, *852*, 73 – 81.

[25] Joshi, J. B., Elias, C. B., Patole, M. S., Role of hydrodynamic shear in the cultivation of animal, plant and microbial cells. *Chem. Engin. J.* 1996, *62*, 121 – 141.

[26] Ho, Ch. S., Oldshue, J. Y., *Biotechnology Processes. Scale-Up and Mixing.* 1987, *AIChE*, New York, NY 1987.

[27] Namdev, P. K., Thompson, B. G., Ward, D. B., Gray, M. R., Effects of glucose fluctuations on synchrony in fed-batch fermentation of *Saccharomyces cerevisiae. Biotechnol. Prog.* 1992, *8*, 501.

[28] Rouf, S. A., Douglas, P. L., Moo-Young, M., Scharer, J. M., Computer simulation for large scale bioprocess design. *Biochem. Engin. J.* 2001, *8*, 229 – 234.

For further reading:

van'Riet, K., Tramper, J., *Basic Bioreactor Design*, Marcel Dekker, New York 1991.

Zhang, S., Chu, J., Zhuang, Y., *Adv. Biochem. Eng. Biotechnol.* 2004, *87*, 97 – 150.

Cabral, J. M. S., Mota, M., Tramper, J., *Multiphase Bioreactor Design*, Taylor & Francis, London, UK 2001.

Blanch, H. W., Clark, D. S., *Biochemical Engineering*, Marcel Dekker, New York, NY 1995.

Leib, T. M., Pereira, C. J., Villadsen, J., Bioreactors: a chemical engineering perspective. *Chem. Engin. Sci.* 2001, *56*, 5485 – 5497.

Vrabel, P., van der Lans, R. G. J. M., Luyben, K. C. A. M., Boon, L., Nienow, A. W., Mixing in large-scale vessels stirred with multiple radial or radial and axial up-pumping impellers: modeling and measurements. *Chem. Eng. Sci.* 2000, *55*, 5881 – 5896.

Schmid, A., Kollmer, A., Mathys, R. G., Witholt, B., Developments toward large-scale bacterial bioprocesses in the presence of bulk amounts of organic solvents. *Extremophiles* 1998, *2*, 249 – 256.

Mavituna, F., Strategies for bioreactor scale-up. *NATO ASI Series*, Series E: Appl. Sci. 1996, *305* (Computer and Information Science Applications in Bioprocess Engineering), 125 – 142.

Schügerl, K., *Bioreaction Engineering, Vol. II, Characteristic Features of Bioreactors*, John Wiley & Sons, Chichester 1991.

Schügerl, K., *Bioreaction Engineering, Vol. I, Fundamentals, Thermodynamics, Formal Kinetics, Idealized Reactor Types and Operation Modes*, John Wiley & Sons, Chichester 1985.

